RESEARCH ARTICLE

GCB-BIOENERGY
BIOPRODUCTS FOR A SUSTAINABLE BIOECONOMY   WILEY

Uncertain effectiveness of *Miscanthus* bioenergy expansion for climate change mitigation explored using land surface, agronomic and integrated assessment models

Emma W. Littleton[1,2,3] 🟢 | Anita Shepherd[4] 🟢 | Anna B. Harper[1,3] 🟢 |
Astley F. S. Hastings[4] 🟢 | Naomi E. Vaughan[5] 🟢 | Jonathan Doelman[6] 🟢 |
Detlef P. van Vuuren[6] 🟢 | Timothy M. Lenton[1,2] 🟢

[1]Global Systems Institute, University of Exeter, Exeter, UK

[2]College of Life and Environmental Sciences, University of Exeter, Exeter, UK

[3]College of Engineering, Mathematics and Physical Sciences, University of Exeter, Exeter, UK

[4]Institute of Biological and Environmental Sciences, School of Biological Sciences, University of Aberdeen, Aberdeen, UK

[5]Tyndall Centre for Climate Change Research, School of Environmental Sciences, University of East Anglia, Norwich, UK

[6]PBL Netherlands Environmental Assessment Agency, The Hague, Netherlands

Correspondence
Emma W. Littleton, Global Systems Institute, University of Exeter, Exeter, UK.
Email: e.w.littleton@exeter.ac.uk

Abstract

Large-scale bioenergy plays a key role in climate change mitigation scenarios, but its efficacy is uncertain. This study aims to quantify that uncertainty by contrasting the results of three different types of models under the same mitigation scenario (RCP2.6-SSP2), consistent with a 2°C temperature target. This analysis focuses on a single bioenergy feedstock, *Miscanthus × giganteus*, and contrasts projections for its yields and environmental effects from an integrated assessment model (IMAGE), a land surface and dynamic global vegetation model tailored to *Miscanthus* bioenergy (JULES) and a bioenergy crop model (MiscanFor). Under the present climate, JULES, IMAGE and MiscanFor capture the observed magnitude and variability in *Miscanthus* yields across Europe; yet in the tropics JULES and IMAGE predict high yields, whereas MiscanFor predicts widespread drought-related diebacks. 2040–2049 projections show there is a rapid scale up of over 200 Mha bioenergy cropping area in the tropics. Resulting biomass yield ranges from 12 (MiscanFor) to 39 (JULES) Gt dry matter over that decade. Change in soil carbon ranges from +0.7 Pg C (MiscanFor) to −2.8 Pg C (JULES), depending on preceding land cover and soil carbon. 2090–99 projections show large-scale biomass energy with carbon capture and storage (BECCS) is projected in Europe. The models agree that <2°C global warming will increase yields in the higher latitudes, but drought stress in the Mediterranean region could produce low yields (MiscanFor), and significant losses of soil carbon (JULES and IMAGE). These results highlight the uncertainty in rapidly scaling-up biomass energy supply, especially in dry tropical climates and in regions where future climate change could result in drier conditions. This has important policy implications—because prominently used scenarios to limit warming to 'well below 2°C' (including the one explored here) depend upon its effectiveness.

---

1 | INTRODUCTION

1.1 | Rationale

To limit global mean temperature increase to 1.5°C above preindustrial levels, net global greenhouse gas emissions should approach zero by 2050 (UNFCCC, 2015). This implies major reductions in greenhouse gas emissions as well as active greenhouse gas removal from the atmosphere to negate emissions sources that cannot be fully mitigated. With a limited carbon budget remaining for the next few decades (Rogelj et al., 2015), biomass is important both as a versatile energy source (e.g. used for heat and electricity production and transport fuels) and as a feedstock for bioenergy with carbon capture and storage (BECCS) to actively remove large amounts of carbon dioxide (CO_2) from the atmosphere (Daioglou et al., 2019). Bioenergy features prominently in many future energy system scenarios, both with and without carbon capture and storage (CCS). BECCS is essential to the most ambitious climate change pathways (Riahi et al., 2017) because it offers the ability to actively reduce atmospheric CO_2 concentration. Future climate scenarios usually feature increasing use of biomass energy as a substantial and important component of total energy, in quantities significantly exceeding current supply (Rogelj et al., 2015; Vaughan et al., 2018).

'Second-generation' bioenergy crops, comprising lignocellulosic perennial grasses, tree species managed as short-rotation coppice or short rotation forestry, and residues from forestry and agriculture, are preferred candidates to meet future biomass energy demand, due to low input requirements and ability to tolerate poor soils (Chum et al., 2011; Valentine et al., 2011).

Most 2°C or lower scenarios feature BECCS being rolled out at scale in the next 10–20 years (Fuss et al., 2014) with bioenergy crops delivering 100–400 EJ year^{-1} (primary energy) by 2100 (Huppmann et al., 2018). The impacts of large-scale bioenergy production on the land surface and Earth system could be significant: changes to vegetation cover across the Earth can change climate systems through biophysical effects such as changes to albedo, evaporation and runoff, or through biogeochemical effects like disturbance or priming of soil carbon (Fontaine et al., 2004). These changes are variable; for example, bioenergy crops can impact albedo and water supplies negatively if timber biomass is sourced from forested areas affected by seasonal snow cover (Cherubini et al., 2012), whereas perennial bioenergy grasses have a higher albedo than annual row crops and if replacing conventional arable agriculture in large areas, could lead to regional cooling and slower snowmelt (Miller et al., 2015).

This research examines the yield potential and soil carbon impacts of large-scale *Miscanthus* production using three types of model: a crop growth model dedicated to *Miscanthus* (MiscanFor), a Dynamic Global Vegetation Model (DGVM; named JULES), and an Integrated Assessment Model (IAM; named IMAGE). This study uses *Miscanthus* as a model bioenergy crop because it produces very high yields under ideal circumstances, but also produces reliably good yields on poor soils with low inputs, and is therefore a very attractive option for meeting high demand for biomass with minimal resource use.

Dedicated bioenergy crop models may be used to project yields and responses to environmental stressors at site or regional level (Robertson et al., 2015). MiscanFor (Hastings, Clifton-Brown, Wattenbach, Mitchell, & Smith, 2009; Shepherd, Littleton, et al., 2020) is an agricultural crop growth model, parameterized for *Miscanthus × giganteus*, that has been applied at UK (Hastings et al., 2014), European (Hastings, Clifton-Brown, Wattenbach, Stampfl, et al., 2009) and global scale (Pogson et al., 2013; Shepherd, Littleton, et al., 2020). These models have a local representation of soil carbon cycling, hydrology and climate and represent crop phenology, growth and their interaction with the soil both in terms of water use, carbon and nutrient cycling. They are not interlinked to global cycles but require monthly weather/climate datasets as inputs when used spatially or for future climates (Hastings et al., 2008).

DGVMs, by contrast, are models specifically developed to address questions about large-scale natural vegetation patterns and productivity, and their links with the climate and Earth system (Sitch et al., 2008) but are less developed in cropping processes. They can be included in Earth system models (ESMs), which enables simulations of large-scale land-use change (such as bioenergy cropland expansion) and evaluation of the biogeophysical and biogeochemical climate impacts of land-use change, including representation of plant growth and soil carbon cycling. However, this typically occurs at the expense of representation of specific plant species and detailed site and management information. There are differences between DGVMs in representation of bioenergy crops and calculation of harvests (Krause et al., 2019). Although some DGVMs, such as JULES, feature explicit representation of bioenergy crops and harvesting (Littleton et al., 2020), others use

approximations based on generic plant functional types (PFTs) and calculate harvests as a fixed proportion of productivity (Muri, 2018).

IAMs are models that combine a socio-economic representation of the human system with a simplified representation of the environment. They are often applied to develop global change pathways, for example, on climate change mitigation, which includes spatial–temporal bioenergy crop scenarios subject to prescribed targets and constraints. They typically use simplified representations of the climate and land surface systems. IMAGE is an IAM that uses crop yields from the DGVM LPJmL (Schaphoff et al., 2018) when determining biomass supply for bioenergy.

1.2 | Aims and objectives

Bioenergy crop expansion raises a number of questions about the feasibility of net negative emissions and their impacts on human and natural systems. No single model addresses all feasibility constraints, trade-offs and co-benefits, so this study utilizes three different types of model, often used independently and in separate disciplines. The results focus on yields and soil carbon as two crucial factors that will determine the effectiveness of BECCS. The discussion includes consideration of the energy and economic system changes that lead to the expansion of bioenergy cropland, to put the projected changes into the context of the SSP2 storyline. Differing projections between the models (all of which have been independently verified) indicates the uncertainty in the effectiveness of large-scale expansion of bioenergy crops to deliver negative emissions.

Cross-genre model inter-comparison is inherently challenging, but can offer valuable insights into complex problems such as the nexus between land availability, biomass yields and carbon cycle response. This study aims to examine the projected response of different modelling approaches to the same scenario of bioenergy land-use expansion, derived from the IMAGE IAM. First, the sensitivity and performance of the three models to present-day data from Europe are compared. Future projections use the SSP2- RCP2.6 mitigation scenario, which aims to achieve <2°C global warming under a socio-economic scenario following established social, economic and technological trends. The yield patterns and soil carbon changes are explored across the three models, with a focus on two particular cases: the tropics in the 2040s, and Europe in the 2090s. Yield and soil carbon projections have been chosen as focal outputs, given that they are key determinants of the overall life cycle carbon balance and the two variables are a common output of all three models.

Figure 1 conceptualizes the foci of the three models in this study. Each model explores the Earth, energy and agronomic systems from different angles while generating output for some of the same variables. In the centre of the diagram are yield and soil carbon change, the two variables simulated by all three models, which are explored in this research.

2 | MATERIALS AND METHODS

2.1 | Models used

Table 1 lists the essential attributes for the model configurations and databases used for this study.

2.2 | IMAGE

IMAGE is an integrated assessment model, incorporating a global energy system model, the LPJml dynamic global vegetation model (DGVM) and the MAGICC simple climate model (Meinshausen et al., 2011). IMAGE 3.0 uses the LPJmL model which dynamically simulates plant growth and agricultural productivity, and the carbon and water dynamics of agricultural land with processes of photosynthesis, respiration, growth and phenology (Stehfest et al., 2014). Management is approximated per crop type on the regional scale. For *Miscanthus*, a plant functional type of a fast-growing annual grass is used (Beringer et al., 2011).
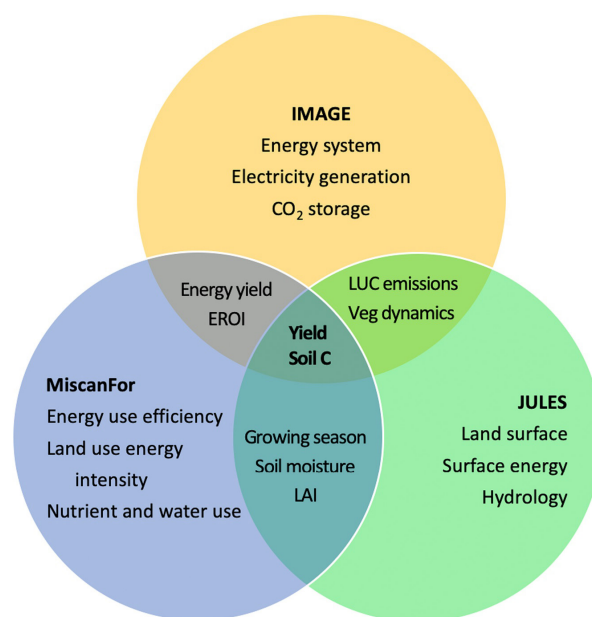

FIGURE 1 Conceptual diagram of the overlaps and unique features of outputs available from the three global land models discussed in this study. Abbreviations used in figure: LUC, land-use change; LAI, leaf area index; EROI: Energy return on investment.

TABLE 1 Comparison of scope of the models used in this study

MODELS	MiscanFor	JULES	IMAGE
Boundary of system processes	Energy crop and associated agronomic system	Land surface, terrestrial vegetation	Socio-economic Energy system
Spatial resolution	5 arc-minutes	30 arc-minutes	30 arc-minutes
Output timestep	10-year mean	1 year	5 years
Extent	Global	Global	Global
Soil PROPERTIES	IGBP[a]	HWSD[b]	HWSD[b]
CLIMATE PROJECTION	HadGEM2-ES RCP 2.6	HadGEM2-ES RCP 2.6	MAGICC in line with RCP 2.6– gridded downscaling based on HadGEM2-ES
BIOENERGY Land USE	IMAGE SSP2	IMAGE SSP2	IMAGE SSP2
CROP SIMULATED	*Miscanthus×giganteus*	*Miscanthus × giganteus*	Plant functional type of *Miscanthus* species

[a]IGBP (international Geosphere-Biosphere Programme; global soil data task, 2000).

[b]HWSD (harmonized world soil database; Fischer et al., 2008).

Agricultural land-use patterns are determined with a land-use allocation algorithm, driven by demographic changes to food demand and using crop productivity, population density, slopes and accessibility to allocate new agricultural land as required (Doelman et al., 2018). Other management practices are calculated internally in LPJmL, such as sowing dates and the demand for irrigation water. The energy system model of IMAGE determines demand for bioenergy per world region based on developments in the energy system, trade patterns and climate change policy (Daioglou et al., 2019). Production of bioenergy is then allocated to the grid level within each region based on relative productivity and sustainability assumptions implying that allocation on carbon-rich ecosystems such as forest is excluded. LPJmL simulates yields per crop under optimal management intensities for each grid cell, which is input to the IMAGE Land-use model for simulations of land-use change dynamics. The physical yield potential is then multiplied by a management factor to obtain the actual projected yield used in this study. The management factor is set separately for each of the 26 IMAGE world regions (Stehfest et al., 2014) and updated annually. This parameter is based on data and assumptions of current practice and technological change in agriculture and is modified in the agro-economic model. Climate change calculated by the IMAGE climate model modifies future agricultural productivity because these components are dynamically linked in annual timesteps. During the period 2040–2049, IMAGE assumed a management factor of 0.8, meaning relatively low efficiency in converting productivity to yield, or yield to energy feedstock, whereas the management factor is 1.4 in Europe by 2090–2099, assuming an increase in yield. The LPJmL module on crop growth directly interacts with the modules on terrestrial carbon and water cycles; as they are all an integral part of the LPJmL model, sharing the same soil and water balance processes.

2.3 | MiscanFor

MiscanFor is a bioenergy crop growth and environmental system model that for this study is parameterized for *Miscanthus×giganteus* (*M×g*) (Hastings, Clifton-Brown, Wattenbach, Stampfl, et al., 2009). It is a daily timestep mechanistic process-based simulation requiring soil and climate databases as input. The model calculates LAI and aboveground biomass during the growing season; post-growing season senescence is represented by leaf litter (providing input to soil carbon) and nutrient repartition to the rhizome. MiscanFor outputs annual spring senesced dry harvest yield of a mature crop after the 3-year establishment period. The annual crop yield is averaged over a decade and includes years of zero crop yield if the crop is killed by drought or frost and has to be re-planted and re-established. In this study, the model outputs mean yields for 10-year time periods, on a grid cell basis globally. Evapotranspiration, radiation use efficiency and leaf area index (LAI) incorporate downregulation factors related to water availability at which transpiration, photosynthesis and leaf expansion slows. Dry matter assimilate is simulated from the fraction of radiation intercepted by the canopy (dependant on LAI, an extinction coefficient, and photosynthetically active radiation), modified by radiation use efficiency, water availability and overheating factors. There is an accounting process for continuously high soil water deficit and low temperature thresholds which kill the crop (60 days below −7°C and 60 days below permanent wilting point), and reduced assimilate production over a threshold for leaf overheating of 28°C. There are six phenological stages of crop development and dormancy. MiscanFor contains a Penman-Monteith evapotranspiration procedure (FAO method, Allen et al., 1998), a soil and litter decomposition module (Dondini et al., 2009), downregulation of photosynthesis with water

scarcity, and a soil carbon decomposition module (for details, see Shepherd, Littleton, et al., 2020). These simulations assume no irrigation and represent rainfed crops with no groundwater support.

2.4 | JULES

The Joint UK Land Environment Simulator (JULES) is a community land surface model that can be run standalone (as described here) or used as the land surface component of the Met Office's Earth System models (Collins et al., 2011). The vegetation and carbon cycle processes of JULES are described in Clark et al. (2011). JULES calculates the surface energy and water fluxes, along with gross and net primary productivity, on an hourly timestep. The net primary productivity (NPP) for each plant functional type (PFT) is accumulated during each timestep, to be later used for calculating changes in vegetation structure and coverage in TRIFFID, the dynamic global vegetation model built into JULES. TRIFFID is called at the end of a user-defined number of days (a 10-day period is used for this study), and the accumulated NPP is allocated between 'growth' and 'spreading'. The former is used for increasing leaf area index (LAI) and canopy height, while the latter is used to allow PFTs to take up more space in a grid cell. Competition for space is determined based on PFT heights: the tallest plants get first access to space in a grid cell, but may not be able to compete if their NPP is too low. A constant background litter flux and litter due to disturbances such as deforestation are added to the soil carbon pool at the end of each TRIFFID timestep. Soil respiration is calculated from four pools with different decay rates.

The version used here is a specialized branch of JULES vn5.1, referred to as JULES-BE. These modifications incorporate a new bioenergy crop PFT representing *Miscanthus*, with additional functionality to allow for periodic harvest of bioenergy crops and for the fractional coverage of bioenergy crops to expand when the area available to them increases. These modifications are described in detail in Littleton et al. (2020).

2.5 | Scenario and simulation development for models

All three models use a single climate and social development pathway: SSP2-RCP2.6. SSP2 is a 'middle of the road' scenario assuming medium challenges to mitigation (medium economic and population growth with a balanced mix of fossil and renewable technologies) and medium challenges to adaptation (Riahi et al., 2017). As a component of the SSP2-RCP2.6 scenario implementation

in IMAGE, the maps of bioenergy crop expansion are produced which are used to define the land used for bioenergy crops in all three models used in this study (Doelman et al., 2018). SSP2-RCP2.6 is described as giving a 66% chance of holding global mean temperature below 2°C above preindustrial levels. In the SSP2 land-use scenario generated by IMAGE, global bioenergy cropping area expands rapidly in the 2020s and 2030s, with a maximum expansion rate of 24 Mha year^{-1} during 2035–2040, reaching a peak near 300 Mha by 2040 (Figure 2a). This analysis focused on two main time periods and regions—an initial period of expansion in the tropics in the 2040s (Table 2; Figure 2b) and later Europe in the 2090s (Figure 2c)—because they illustrate the two main purposes of 21st century bioenergy in ambitious climate change mitigation scenarios: as an inexpensive way to scale up renewable energy supply and later as a sustainable feedstock for BECCS (Table 2) (Daioglou et al., 2019; Rogelj et al., 2015).

The meteorological driving data for MiscanFor and JULES were based on HadGEM2-ES RCP2.6 from the ISIMIP project (Hempel et al., 2013), where original HadGEM2-ES outputs were downscaled to 0.5°×0.5° and bias-corrected to calibrate with WATCH observed climatology over 1960–1999 to produce a climate time series from 2006 to 2099. IMAGE uses a climate change pathway in line with RCP 2.6 as calculated by MAGICC which is downscaled to the grid level using HadGEM2-ES data from the ISIMIP project. The mean temperature increase for this pathway in the suite of CMIP5 models is 1.6°C above 1850–1900 levels (Collins et al., 2013). The RCP2.6 scenario (van Vuuren et al., 2011) features strong mitigation action, with global CO_2 emissions peaking in 2020 and declining to zero by 2080. This is facilitated by an increasing price on greenhouse gas emissions which incentivizes bioenergy with carbon capture and storage (BECCS), as well as bioenergy without CCS (BE) for decarbonizing energy supply. This climate scenario is used because of its strong use of bioenergy and BECCS, which is consistent with the land-use change in the IMAGE SSP2-RCP2.6 scenario used in this study, while the bias-correction of HadGEM2-ES output enables this comparison of present-day yields to observations.

3 | RESULTS

3.1 | Comparison to present-day observations

Figure 3 shows how the three models compare in Europe against observations collected between 1980 and 2011 (Li et al., 2018) for *Miscanthus* yield. The models show a similar range of potential yields across Europe (mean±1SD, tonnes DM ha^{-1} year^{-1}: MiscanFor: 9.7±6.3; JULES:
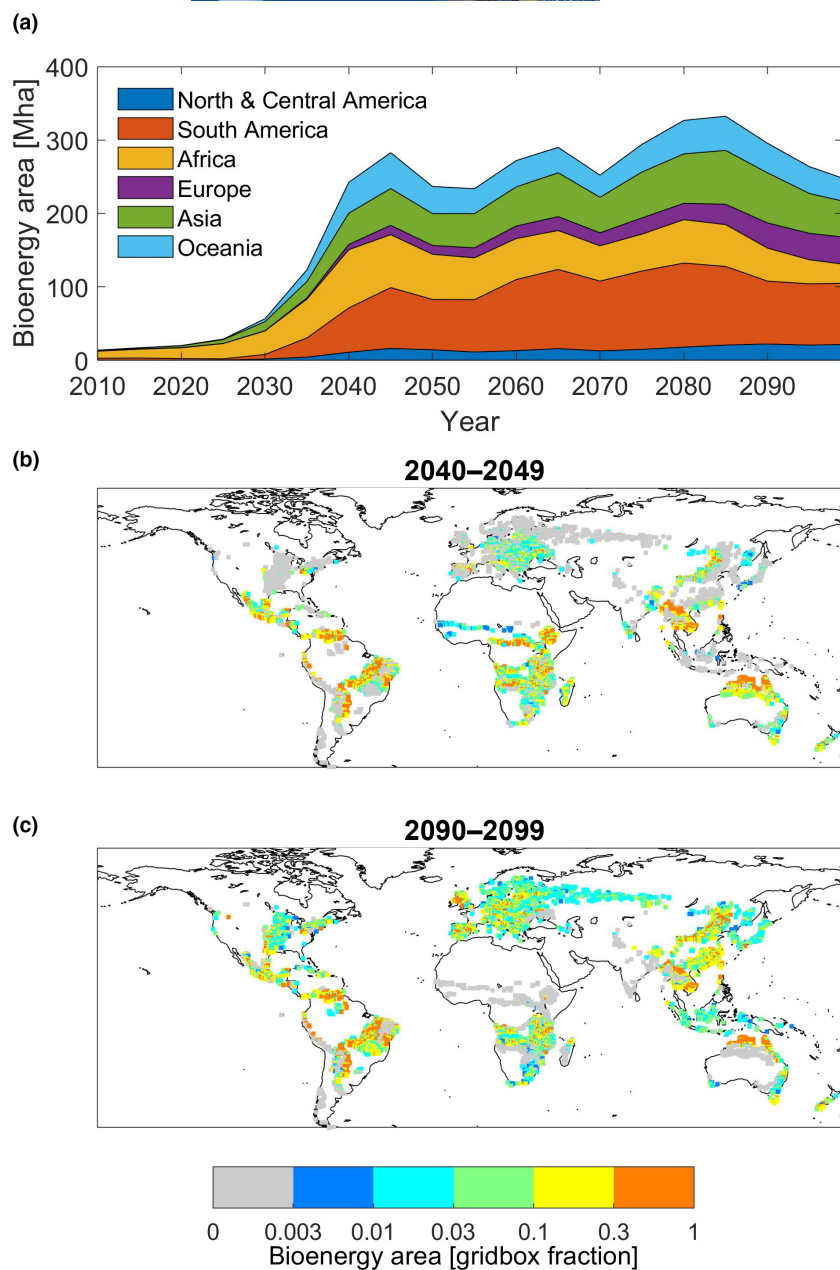
(a)

(b)

(c)

FIGURE 2 (a) Bioenergy crop area progression by continent in this study (RCP2.6-SSP2), over 2010–2100. Geographical distribution of bioenergy crop area in (b) 2040s and (c) 2090s.

	Tropics (lat < 25°N/S)	Europe (lat > 35°N, 15°W < lon < 40°)
Land area for BE crops	245 Mha (2045 snapshot)	34 Mha (2095 snapshot)
Land area converted to BE crops over period	218 Mha (2025–2045)	13 Mha (2075–2095)
% of BE in total primary energy	26% (2040 snapshot)	48% (2090 snapshot)
% of BECCS in total BE	19% (2040 snapshot)	69% (2090 snapshot)

TABLE 2 Features of the two bioenergy narratives explored in this study

11 ± 4.8; IMAGE: 8.3 ± 4.5), although with different patterns. Comparing only the grid cells with observations (Figure 3a), none of the models simulated yields over 20 t dry matter yield (DM) ha^{-1} year^{-1}, compared to two observed sites in southern Europe where yields averaged between 20 and 25 t DM ha^{-1} year^{-1}. Each model has

regions it simulates more and less accurately. High yields have been observed at a few locations in southern Europe which JULES and IMAGE simulate but MiscanFor does not. The west of UK has higher observed yields than the east due to higher precipitation; MiscanFor simulates this, whereas JULES and IMAGE miss this effect. Figure 3b
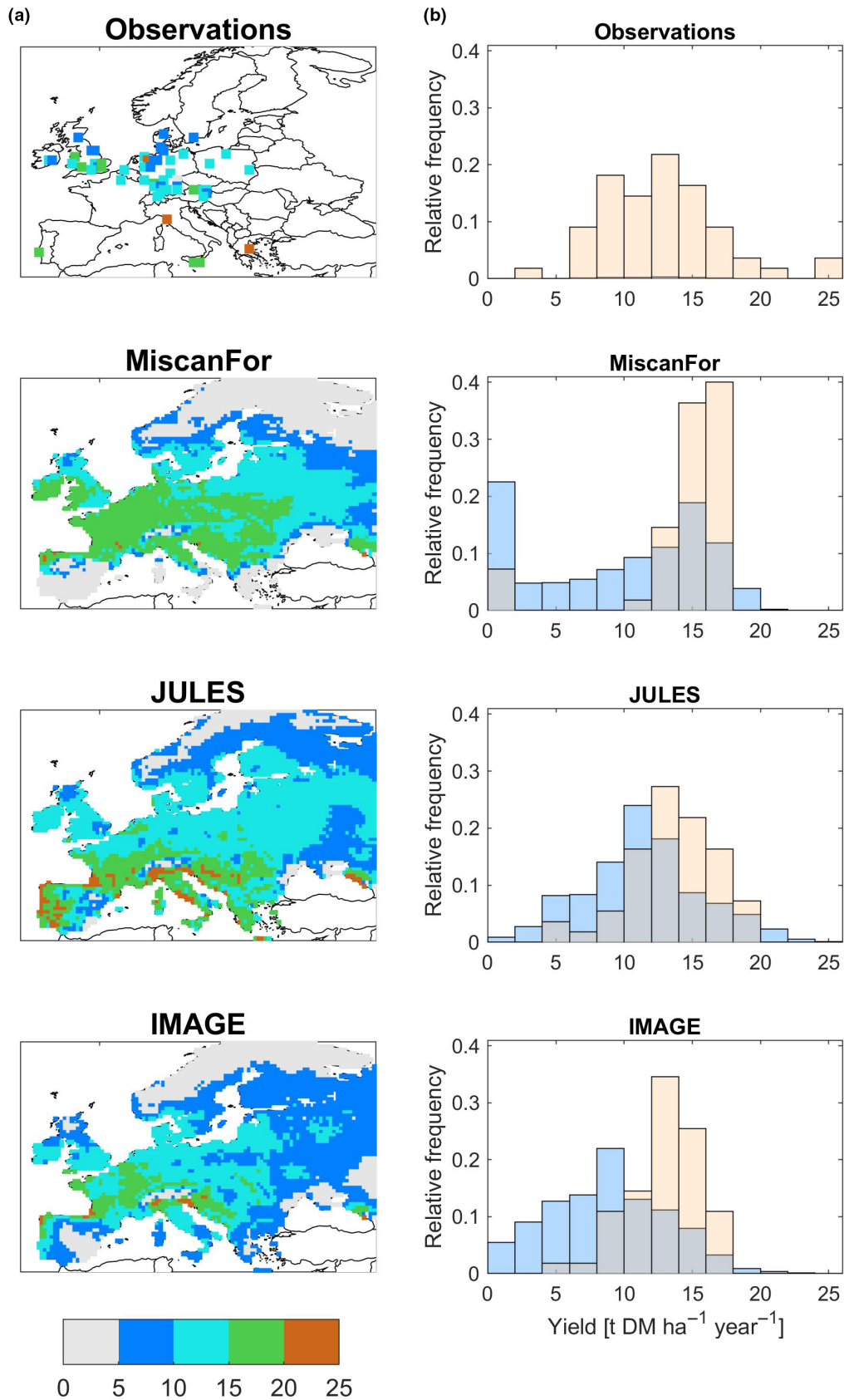
FIGURE 3 Bioenergy crop yield across Europe from MiscanFor, JULES and IMAGE, for the 2010–2019 period, compared to observations collated by Li et al. (2018): (a) mapped values, (b) plotted peaks.

shows that MiscanFor has a narrower distribution of yield than the other models over Europe.

3.2 | The tropics 2040–2049: Yield and soil carbon

From 2025 to 2045, approximately 200 Mha of land in the tropics is converted to grow bioenergy crops in the SSP2-RCP2.6 scenario (Table 2). The three models project very different future *Miscanthus* yields in the tropics during 2040–2049. MiscanFor yields are modest and are generally less than 10 t DM ha^{-1} year^{-1} (mean ± 1SD: 4.7 ± 4.5). IMAGE projects higher yields, especially in Indonesia where yields are over 20 t DM ha^{-1} year^{-1} (mean ± 1SD: 9.0 ± 4.7). JULES projects the highest yields, with some locations yielding over 25 t DM ha^{-1} year^{-1} across the tropics (mean ± 1SD: 16.6 ± 8.2). These differences primarily result from the different ways that plant productivity depends on leaf temperature and soil moisture across the three models.

All three models display stronger correlations between yield and Mean Annual Precipitation (MAP) than between yield and Mean Annual Temperature (MAT) (Figure S1) for the climate of this region. The relationship with MAP is strongest in IMAGE ($r^2 = 0.51$), and weaker in JULES ($r^2 = 0.40$) and MiscanFor ($r^2 = 0.34$). Figure S2 shows that the MiscanFor model is sensitive to a decrease in precipitation more than an increase, and is more sensitive to field capacity and wilting point. It is therefore the water-holding capacity of the soils that has a more pronounced relationship with yield. MiscanFor's radiation use efficiency parameters for *Miscanthus × giganteus* (used for this simulation) model a decrease in growth rate when temperatures exceed 30°C but not for other genotypes.

Table 3 shows the soil carbon change. The processes used by each model for calculating soil carbon exert a strong influence on projections of future change in soil carbon. In MiscanFor, the signal is almost entirely positive, with a nearly linear relationship with yield (Figure S4). MiscanFor is an agricultural model. Unlike the other models which are built for natural vegetation, it is built to process agricultural and wasteland low-grade soils. It imports initial total soil carbon from the IGBP (Global Soil Data Task Group, 2000) soil database values and has 2 years of spin-up for the soil water content and soil decomposition to be initiated before crop residue accumulates. This result reflects the change in soil carbon per hectare for land-use change from cropland/grassland to bioenergy cropland using the initial SOC from the IGBP spatial maps, not peatlands and forests. See Shepherd, Littleton, et al. (2020) for details of the Bosatta and Agren's (1985, 1991) method of soil carbon decomposition. In JULES and IMAGE, the

TABLE 3 Soil carbon change relating to bioenergy expansion. Values are the difference between the end of the studied decade (tropics 2049, Europe 2099) and the start (tropics 2039, Europe 2089)

Soil C change over:	The tropics 2040–2049 (lat < 25°N/S)	Europe 2090–2099 (lat > 35°N, 15°W < lon < 40°E)
MiscanFor	+670 Mt C [+ 0.3 t C ha^{-1} year^{-1}]	+80 Mt C [+ 0.2 t C ha^{-1} year^{-1}]
JULES	−2830 Mt C [− 1.2 t C ha^{-1} year^{-1}]	−210 Mt C [− 0.6 t C ha^{-1} year^{-1}]
IMAGE	−700 Mt C [− 0.3 t C ha^{-1} year^{-1}]	−29 Mt C [− 0.1 t C ha^{-1} year^{-1}]

picture is more complicated, because they simulate land cover change dynamics over whole grid cells, of which only a small fraction is usually given to bioenergy crops (Figure 2), so the correlation between bioenergy area and soil carbon change is generally weak over the whole grid cell. However, a small negative trend in soil carbon is apparent in the most heavily cropped sites (Figure S3).

Figure 5 shows soil carbon change (t C ha^{-1} year^{-1}) of bioenergy crop area only. Although MiscanFor is predominantly just over zero, and JULES and IMAGE are predominantly just under zero, there is not a large difference in the rate of soil carbon change. However, a small difference in the rate of soil carbon change between models over such large areas (shown in Table 2) gives rise to very large cumulative values and differences (Table 3; Figure S5).

3.3 | Europe, 2090–2099

Figure 6 displays the projected yields of *Miscanthus* in Europe averaged over 2090–2099. The models appear to agree broadly (mean ± 1SD, tonnes DM ha^{-1} year^{-1}: MiscanFor: 11.1 ± 4.9; JULES: 10.9 ± 2.9; IMAGE: 8.8 ± 2.4); however, some important spatial differences are apparent. As in Figure 4, MiscanFor shows a stronger response to dry climates with yields of <5 t DM ha^{-1} year^{-1} in southern Europe; JULES indicates stronger yields in these regions, with IMAGE showing a more mixed response. By contrast, MiscanFor shows higher yields than the other two models in central Europe and Wales. Increasing global temperatures averaging 2°C (higher in temperate northern hemisphere; higher over land) mean that yields will increase at higher latitudes, meanwhile lower latitudes with drier Mediterranean summers reduce yields—MiscanFor is most sensitive to changes in precipitation via the available water capacity of soils (Figure S2). All models are sensitive to precipitation to some degree (Figure S1); MiscanFor, more than the other two models, projects severely reduced crop yields with water stress. Since there is so much uncertainty in these precipitation
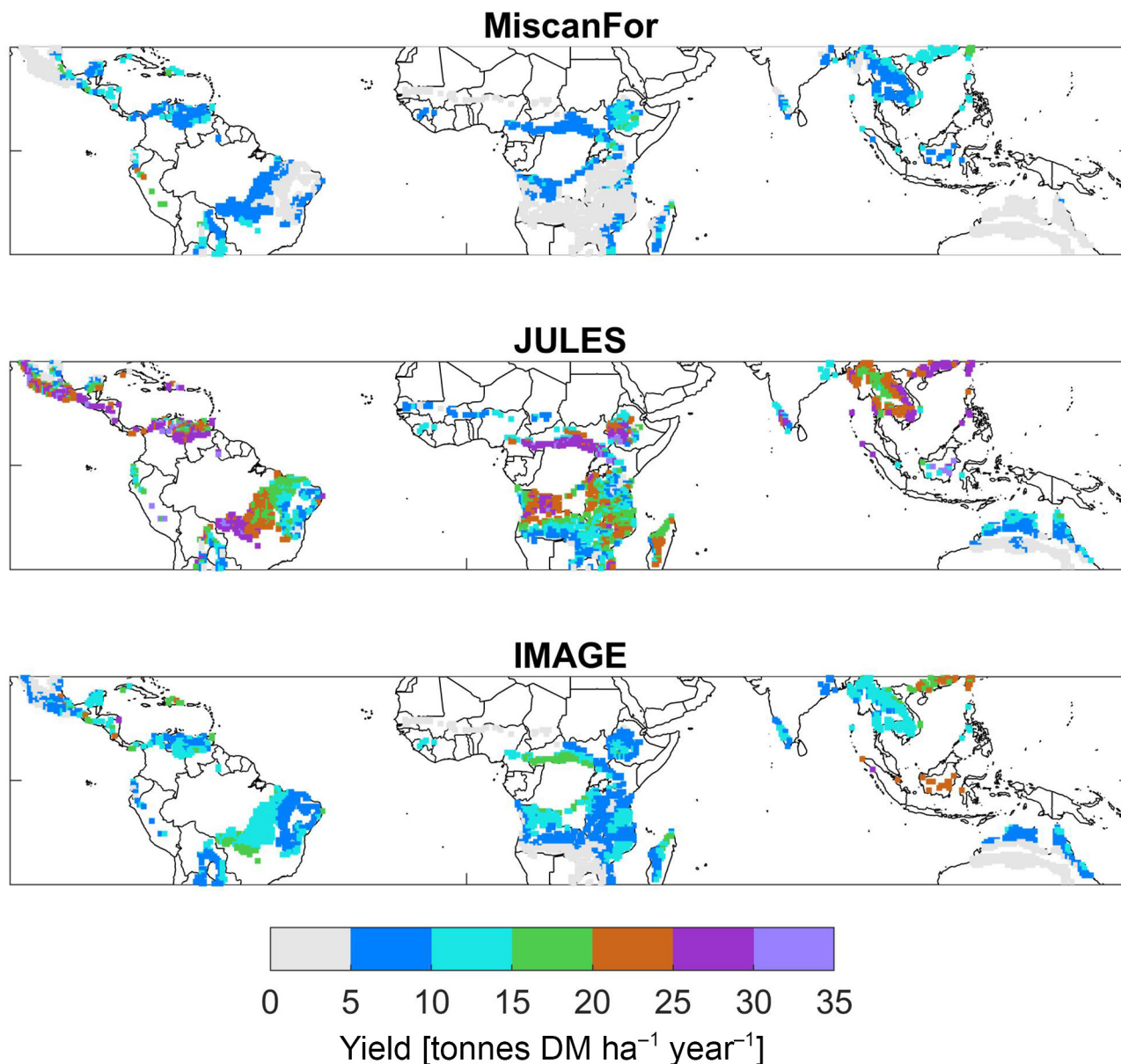
MiscanFor

JULES

IMAGE

FIGURE 4 The tropics yield 2040–2049, t dry matter yield ha^{-1} year^{-1}.

patterns, it would be interesting to assess variation in climate ensembles (shown for MiscanFor in a paper focusing on the uncertainty of input data, Shepherd, Martin, & Hastings, 2020).

For the historic simulation period 2010–2019 (Figure 3), MiscanFor was the only model to detect higher yields for the wetter UK west coast, whereas in Figure 6, all models under RCP2.6 show higher yields for the west coast compared to no yield in the south and east. In the 2090–2099 period, the climate will have changed, and MiscanFor yields are generally as high or higher over the map than JULES and IMAGE. IMAGE increases its management or yield efficiency factor to 1.4 in Europe by the 2090s (compared to 0.8 in the present day), under the assumption that bioenergy yields can be increased with improved crop

breeding, technology and management practices. The soil carbon change (Figure 7) is somewhat more favourable here than in the tropics; while still overall positive in MiscanFor and negative in JULES and IMAGE (Table 3), the losses are smaller and many areas show an increase in soil carbon across the three models. This is attributable to higher yields (MiscanFor; Figure 6) and more mixed previous land use (JULES and IMAGE).

4 | DISCUSSION

Despite exploring three different types of model, they likely do not span the uncertainty in actual yields of *Miscanthus*, given that modelled yields are less variable
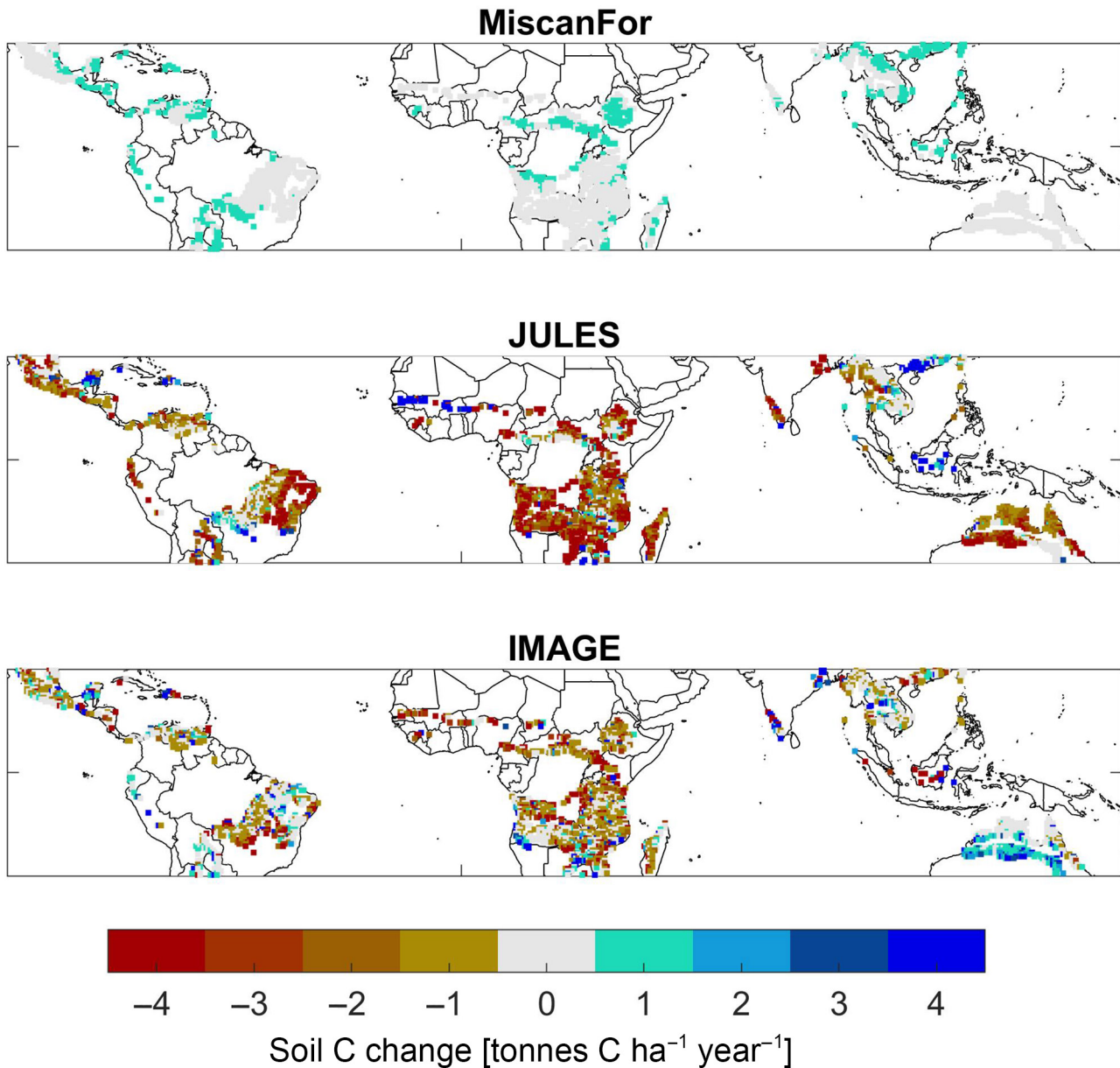
FIGURE 5 The tropics soil carbon change 2040–2049, bioenergy crop area only, t C ha^{-1} year^{-1}.

than observations across Europe. In particular, highest observed yields are not captured. JULES and IMAGE capture more of the variation in yields than MiscanFor, although MiscanFor does capture the possibility of drought dieback. MiscanFor was only run for the current commercial variety of *Miscanthus × giganteus*. JULES *Miscanthus* PFT is tuned using *Miscanthus × giganteus* (Littleton et al., 2020). This variety is optimized for temperate climates and, though the supporting data are sparse, appears to suffer under high temperatures (Davey et al., 2017) and is not very drought tolerant (Clifton-Brown et al., 2002; Scordia et al., 2020). IMAGE uses a generic non-woody biomass plant functional type (Beringer et al., 2011), which is assumed second-generation lignocellulosic, that is, *Miscanthus*, grown

with no irrigation or fertilizer (PBL, 2017). Owing to sparse observations of *Miscanthus × giganteus* in tropical climates, it is difficult to assess the accuracy of modelled yields over much of the world. JULES likely overestimates yield in dry areas as its dieback mechanism is unsophisticated. In contrast, MiscanFor has a very high drought kill in warmer and seasonally arid regions. The models are sensitive to water carrying capacity of the soil, which depends on soil type, and MiscanFor highlights how sensitive yields can be to this. To constrain models run globally, there is clearly a need for more widespread observational studies. This especially true as in many areas there is some groundwater support and there is not a global dataset mapping this feature. Recent modification of MiscanFor (Shepherd, Littleton,
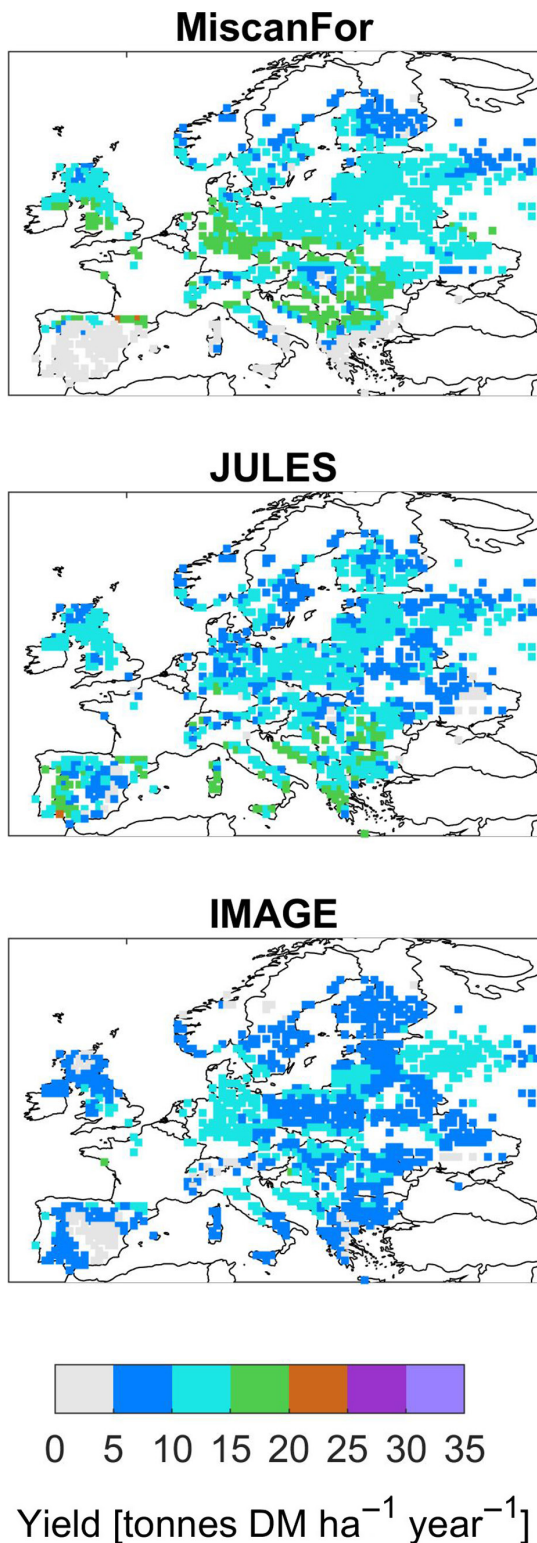
MiscanFor

JULES

IMAGE

FIGURE 6 Europe yield 2090–2099, t dry matter yield ha^{-1} year^{-1}.

MiscanFor

JULES

IMAGE

Soil C change [tonnes C ha^{-1} year^{-1}]

FIGURE 7 Europe change in soil carbon 2090–2099, bioenergy crop area only, t C ha^{-1} year^{-1}.

et al., 2020) uses the parameter for seasonal ground wetness from the HWSD database, and has been used to predict *Miscanthus×giganteus* growth, but this parameter is only currently available for data points that are derived from the European Soil Data Base.
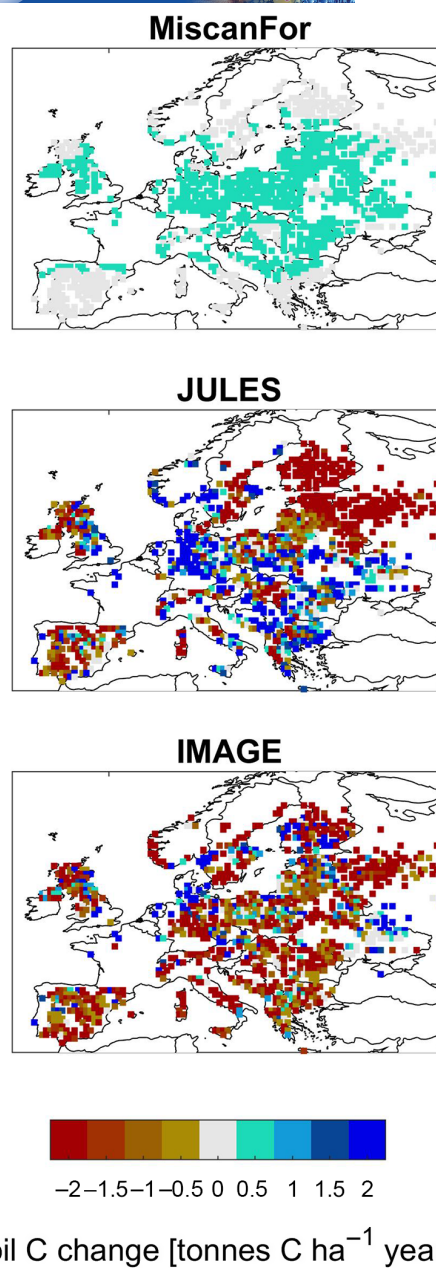
The estimates of biomass production from the rapid scale-up of biomass energy in the tropics by the 2040s differ by a factor of three: cumulative biomass production ranges from 12 (MiscanFor) to 39 (JULES) Gt dry matter over that decade (IMAGE: 22 Gt DM), or assuming a ~50% carbon content ~6–20 Pg C. Soil carbon change over the decade ranges from +0.7 Pg C (MiscanFor) to −2.8 Pg C (JULES). MiscanFor simulates soil carbon increases due to litterfall from *Miscanthus*. The simulated increases compare well to observed increases at sites in Europe (Dondini et al., 2009; Shepherd, Littleton, et al., 2020). JULES includes soil C inputs from leaf,

root and woody biomass litterfall; however, the inputs are parameterized the same for natural grasses and the Miscanthus PFT. In the JULES simulation, soil carbon losses amount to ~15% of biomass production (and average 1.2 t C ha^{-1} year^{-1}). Hence, a significant fraction of the mitigation gains from reducing CO_2 emissions plus any CO_2 removal (BECCS) could be lost. These soil C losses depend on the preceding land cover type and are particularly pronounced in the humid tropics where bioenergy crops (indirectly) replace forests. Large soil carbon losses caused by Miscanthus expansion were also found in JULES and five other DGVMs in Harper et al. ([2018](#)). This brings up an important distinction between the crop model MiscanFor and DGVMs: while MiscanFor simulates only the important and relevant processes that impact soil carbon accumulation at site level, the DGVMs also account for soil carbon losses due to land-use change. The results from MiscanFor in particular indicate that the current commercial clone *Miscanthus×giganteus* will not be a suitable genotype for the dry tropics and other *Miscanthus* varieties (Clifton-Brown et al., [2019](#)) or other crop types including succulents (Mason et al., [2015](#)) could be favoured for bioenergy production in drier, hotter climates.

There is greater agreement across the three models for yields in the 2090s in Europe. This is could be because Europe is the place with most of the observational data against which the models were developed. Cumulative biomass production ranges from 3.0 (IMAGE) to 4.0 Gt DM (JULES) (MiscanFor: 3.7 Gt DM) over the decade. There are still significant differences in soil C response from average gains of 0.2 t C ha^{-1} year^{-1} to losses of −0.6 t C ha^{-1} year^{-1}. Losses of carbon from natural vegetation and soil need to be offset against projected net uptake from BECCS (Harper et al., [2018](#)). Many observational studies have shown that *Miscanthus* cultivation can increase soil carbon on cropland, as represented by MiscanFor in this study. JULES and IMAGE, however, can account for the detail that in this scenario, most of the land is indirectly sourced from natural land, and therefore a decline in soil carbon is evident in two of the three models in the first few decades following this land-use disturbance. This may not be accurate to all situations, and the soil carbon loss may be reversed over subsequent decades of *Miscanthus* cultivation. Better capturing of these dynamics is a target for future development within global land surface models such as JULES.

A key challenge in the SSP2-RCP2.6 scenario is the projected rate of expansion of bioenergy cropping, particularly in the 2040s in the tropics, which in reality would present a major scaling-up challenge. The expansion rate peaks at 24 Mha year^{-1} during 2035–2040. This study has used *Miscanthus* as a sole representative bioenergy crop, but in reality, a mixture of bioenergy crops will likely be grown—especially if such rapid scaling up is attempted and significant crop and agronomy improvements are required to span the geographic and climatic areas proposed in this scenario. The start of the large increase in cropping area projected by IMAGE under the SSP2 socioeconomic scenario is in 2025. Although the IMAGE model represents bioenergy as second generation, lignocellulosic crops, issues like land tenure lengths and short-term market forces currently hamper perennial bioenergy crops in favour of first-generation biofuels which represent lower economic risk to farmers. Hence major near-term growth in bioenergy cropping will more likely be supplied by corn ethanol and palm oil in the tropics—with associated risks to food security (as these typically replace food crops) and associated greenhouse gas emissions from their higher-intensity cropping.

Where and when second-generation lignocellulosic cropping can expand, it is likely to involve a mix of *Miscanthus* and other species and new hybrids, depending on the climate and location. *Miscanthus×giganteus* is sterile and must be propagated by rhizome, placing inherent limitations on its expansion (Clifton-Brown et al., [2019](#)). *Miscanthus* seeded hybrids and other second-generation lignocellulosic crops may be scaled up from seed, and are currently being developed (Clifton-Brown et al., [2019](#); Hastings et al., [2017](#)). However, they do not have the same reliably high yields in poor conditions that *Miscanthus×giganteus* has demonstrated (McCalmont et al., [2017](#)). *Miscanthus* is favoured for its low soil nitrogen emissions and its provision of residue to improve soil carbon where it replaces annual arable crops, and as a perennial it creates a legacy of continuing these processes for many years. Other *Miscanthus*, for example, *Miscanthus sinensis*, do grow well in hot climates (~30 t DM ha^{-1} year^{-1} in China) and other grasses like *Pennisetum purpureum* (elephant grass), *Arundo donax* L. (Giant reed), and *Panicum virgatum* (switchgrass) show promise for growth in warm or arid climates. The future use of a diversity of species may reduce the uncertainty on bioenergy yields that emerges from this intercomparison of three models.

Future scenarios of low-carbon energy systems feature a wide range of estimates of bioenergy contribution, ranging over 75–675 EJ year^{-1} (Bauer et al., [2017](#); Creutzig et al., [2015](#); Slade et al., [2014](#)). This analysis shows that even toward lower end estimates (100–200 EJ year^{-1}), there are serious feasibility concerns. Therefore, these findings support previous constraints on bioenergy (Chum et al., [2011](#)), which suggest that higher ranges, for example, 300–400 EJ year^{-1} and upwards, would be extremely

challenging, presenting significant issues not just socially but also biophysically.

The uncertainty in bioenergy feasibility underscores the necessity of pursuing other more assured climate mitigation actions such as efficiency improvements, reducing consumption further or other renewables (Esmeijer et al., 2018; van Vuuren et al., 2018). Yields compatible with a 2°C emissions profile will require more land area to mitigate carbon emissions if the projected yields are not achieved or if the climate proves more sensitive to CO_2.

Sustainable bioenergy provides significant value to low-carbon energy systems, offering unique potential for BECCS, transport fuels and off-grid applications. However, a sustainable supply of biomass is best considered as a finite and limited resource, as two of the models in this study project substantial carbon losses if bioenergy crops replace natural vegetation and forests (either directly or indirectly). Therefore, biomass energy should be used smartly and carefully, and a well-considered use of land and other resources is critical.

ACKNOWLEDGEMENTS

ORCID

Emma W. Littleton https://orcid.org/0000-0001-5576-5498
Anita Shepherd https://orcid.org/0000-0003-1902-5147
Anna B. Harper https://orcid.org/0000-0001-7294-6039
Astley F. S. Hastings https://orcid.org/0000-0001-9863-7613
Naomi E. Vaughan https://orcid.org/0000-0002-4532-2084
Jonathan Doelman https://orcid.org/0000-0002-6842-573X
Detlef P. van Vuuren https://orcid.org/0000-0003-0398-2831
Timothy M. Lenton https://orcid.org/0000-0002-6725-7498

REFERENCES

Allen, R. G., Pereira, L. S., Raes, D., & Smith, M. (1998). Crop evapotranspiration-Guidelines for computing crop water requirements-FAO Irrigation and drainage paper 56. FAO, Rome, *300*(9), D05109.

Bauer, N., Calvin, K., Emmerling, J., Fricko, O., Fujimori, S., Hilaire, J., Eom, J., Krey, V., Kriegler, E., Mouratiadou, I., Sytze de Boer, H., van den Berg, M., Carrara, S., Daioglou, V., Drouet, L., Edmonds, J., Gernaat, D. E., Havlík, P., Johnson, N., ... Kriegler, E., (2017). Shared socio-economic pathways of the energy sector – Quantifying the narratives. *Global Environmental Change*, *42*, 316–330, ISSN 0959–3780. https://doi.org/10.1016/j.gloenvcha.2016.07.006

Beringer, T., Lucht, W., & Schaphoff, S. (2011). Bioenergy production potential of global biomass plantations under environmental and agricultural constraints. *GCB Bioenergy*, *3*, 299–312. https://doi.org/10.1111/j.1757-1707.2010.01088.x

Bosatta, E., & Agren, G. I. (1985). Theoretical analysis of decomposition of heterogeneous substrates. *Soil Biology and Biochemistry*, *17*, 601–610. https://www.sciencedirect.com/science/article/abs/pii/0038071785900355

Bosatta, E., & Agren, G. I. (1991). Dynamics and carbon and nitrogen in the organic matter of the soil: A generic theory. *The American Naturalist*, *138*, 227–245. https://www.jstor.org/stable/2462541

Cherubini, F., Bright, R., & Strømman, A. (2012). Site-specific global warming potentials of biogenic CO_2 for bioenergy: Contributions from carbon fluxes and albedo dynamics. *Environmental Research Letters*, *7*, 045902. https://doi.org/10.1088/1748-9326/7/4/045902

Chum, H., Faaij, A., Moreira, J., Berndes, G., Dhamija, P., Dong, H., & Pingoud, K. (2011). Bioenergy. In O. Edenhofer, R. Pichs-Madruga, Y. Sokona, K. Seyboth, P. Matschoss, S. Kadner, T. Zwickel, P. Eickemeier, G. Hansen, S. Schlomer, & C. Von Stechow (Eds.), *IPCC special report on renewable energy sources and climate change mitigation* (pp. 209–332). Cambridge University Press. https://www.ipcc.ch/site/assets/uploads/2018/03/Chapter-2-Bioenergy-1.pdf

Clark, D. B., Mercado, L. M., Sitch, S., Jones, C. D., Gedney, N., Best, M. J., Pryor, M., Rooney, G., Essery, R. I., Blyth, E., Boucher, O., Harding, R. J., & Cox, P. M. (2011). The joint UKland environment simulator (JULES), model description – Part 2: Carbon fluxes and vegetation dynamics. *Geoscientific Model Development*, *4*, 701–722. https://doi.org/10.5194/gmd-4-701-2011

Clifton-Brown, J. C., Lewandowski, I., Bangerth, F., & Jones, M. B. (2002). Comparative responses to water stress in stay-green, rapid- and slow senescing genotypes of the biomass crop, *miscanthus*. *New Phytologist*, *154*, 335–345. https://doi.org/10.1046/j.1469-8137.2002.00381.x

Clifton-Brown, J., Harfouche, A., Casler, M. D., Dylan Jones, H., Macalpine, W. J., Murphy-Bokern, D., Smart, L. B., Adler, A., Ashman, C., Awty-Carroll, D., Bastien, C., Bopper, S., Botnari, V., Brancourt-Hulmel, M., Chen, Z., Clark, L. V., Cosentino, S., Dalton, S., Davey, C., ... Lewandowski, I. (2019). Breeding progress and preparedness for mass-scale deployment of perennial

lignocellulosic biomass crops switchgrass, miscanthus, willow and poplar. *Global Change Biology Bioenergy*, *11*, 118–151. https://doi.org/10.1111/gcbb.12566

Collins, W. J., Bellouin, N., Doutriaux-Boucher, M., Gedney, N., Halloran, P., Hinton, T., Hughes, J., Jones, C. D., Joshi, M., Liddicoat, S., Martin, G., & O'Connor, F. (2011). Development and evaluation of an earth-system model – HadGEM2. *Geoscientific Model Development*, *4*, 997–1062. https://doi.org/10.5194/gmdd-4-997-2011

Collins M, Knutti R, Arblaster J, Dufresne J-L, Fichefet T, Friedlingstein P, Gao X, Gutowski W J, Johns T, Krinner G, Shongwe M, Tebaldi C, Weaver A J, Wehner M. (2013). Long-term climate change: Projections, commitments and irreversibility. In: Climate change 2013: The physical science basis. Contribution of Working Group I to the Fifth Assessment Report of the Intergovernmental Panel on Climate Change [Stocker T F, Qin D, Plattner G-K, Tignor M, Allen S K, Boschung J, Nauels A, Xia Y, Bex V, Midgley P M. (eds.)]. Cambridge University Press, Cambridge, United Kingdom and New York, NY, USA.

Creutzig, F., Ravindranath, N. H., Berndes, G., Bolwig, S., Bright, R., Cherubin, F., Chum, H., Corbera, E., Delucchi, M., Fargione, A., Haberl, H., Heath, G., Lucon, O., Plevin, R., Popp, A., Robledo-Abad, C., Rose, S., Smith, P., Stromma, A., ... Masera, O. (2015). Bioenergy and climate change mitigation: An assessment. *GCB Bioenergy*, *7*, 916–944. https://doi.org/10.1111/gcbb.12205

Daioglou, V., Doelman, J. C., Wicke, B., Faaij, A., & van Vuuren, D. P. (2019). Integrated assessment of biomass supply and demand in climate change mitigation scenarios. *Global Environmental Change*, *54*, 88–101. https://doi.org/10.1016/j.gloenvcha.2018.11.012

Davey, C. L., Jones, L. E., Squance, M., Purdy, S. J., Maddison, A. L., Cunniff, J., Donnison, I., & Clifton-Brown, J. (2017). Radiation capture and conversion efficiencies of *Miscanthus sacchariflorus*, *M. sinensis* and their naturally occurring hybrid *M.×giganteus*. *GCB Bioenergy*, *9*, 385–399. https://doi.org/10.1111/gcbb.12331

Doelman, J. C., Stehfest, E., Tabeau, A., van Meijl, H., Lassaletta, L., Gernaat, D. E. H. J., Hermans, K., Harmsen, M., Daioglou, V., Biemans, H., van der Sluis, S., & van Vuuren, D. P. (2018). Exploring SSP land-use dynamics using the IMAGE model: Regional and gridded scenarios of land-use change and land-based climate change mitigation. *Global Environmental Change*, *48*, 119–135. https://doi.org/10.1016/j.gloenvcha.2017.11.014

Dondini, M., Hastings, A., Saiz, G., Jones, M. B., & Smith, P. (2009). The potential of Miscanthus to sequester carbon in soils: Comparing field measurements in Carlow, Ireland to model predictions. *GCB Bioenergy*, *1*(6), 413–425. https://doi.org/10.1111/j.1757-1707.2010.01033.x

Esmeijer K, den Elzen M, Gernaat D, van Vuuren D, Doelman J, Keramidas K, Tchung-Ming S, Després J, Schmitz A, Forsell N, Havlik P, Frank S. (2018). 2°C and 1.5°C scenarios and possibilities of limiting the use of BECCS and bio-energy. PBL Netherlands environmental assessment agency, the Hague. http://pure.iiasa.ac.at/id/eprint/15644/1/pbl-2018-2-degree-and-1-5-degree-scenarios-and-possibilities-of-limiting-the-use-of-beccs-and-bio-energy_3133.pdf

Fontaine, S., Bardoux, G., Abbadie, L., & Mariotti, A. (2004). Carbon input to soil may decrease soil carbon content. *Ecology Letters*, *7*, 314–320. https://doi.org/10.1111/j.1461-0248.2004.00579.x

Fischer, G. F., Nachtergaele, F. O., Prieler, S., van Velthuizen, H. T., Verelst, L., & Wiberg, D. (2008). Global Agro-ecological zones assessment for agriculture (GAEZ 2008). In *FAO*. IIASA and FAO.

Fuss, S., Canadell, J., Peters, G., Tavoni, M., Andrew, R. M., Ciais, P., Jackson, R. B., Jones, C. D., Kraxner, F., Nakicenovic, N., Le Quéré, C., Raupach, M. R., Sharifi, A., Smith, P., & Yamagata, Y. (2014). Betting on negative emissions. *Nature Climate Change*, *4*, 850–853. https://doi.org/10.1038/nclimate2392

Global Soil Data Task Group. (2000). Global Gridded Surfaces of Selected Soil Characteristics (IGBP-DIS). [Global Gridded Surfaces of Selected Soil Characteristics (International Geosphere-Biosphere Programme – Data and Information System)]. Data set. http://www.daac.ornl.gov from Oak Ridge National Laboratory Distributed Active Archive Center, Oak Ridge, Tennessee, U.S.A. 2018. https://doi.org/10.3334/ORNLDAAC/569

Harper, A. B., Powell, T., Cox, P. M., House, J., Huntingford, C., Lenton, T. M., Sitch, S., Burke, E., Chadburn, S. E., Collins, W. J., Comyn-Platt, E., Daioglou, V., Doelman, J. C., Hayman, G., Robertson, E., van Vuuren, D., Wiltshire, A., Webber, C. P., Bastos, A., ... Shu, S. (2018). Land-use emissions play a critical role in land-based mitigation for Paris climate targets. *Nature Communications*, *9*, 2938. https://doi.org/10.1038/s41467-018-05340-z

Hastings, A., Clifton-Brown, J., Wattenbach, M., Stampfl, P., Mitchell, C. P., & Smith, P. (2008). Potential of *miscanthus* grasses to provide energy and hence reduce greenhouse gas emissions. *Agronomy for Sustainable Development*, *28*, 465–472.

Hastings, A., Clifton-Brown, J., Wattenbach, M., Mitchell, C. P., & Smith, P. (2009). The development of MiscanFor, a new miscanthus crop growth model: Towards more robust yield predictions under different climatic and soil conditions. *Global Change Biology Bioenergy*, *1*, 154–170. https://doi.org/10.1111/j.1757-1707.2009.01007.x

Hastings, A., Clifton-Brown, J., Wattenbach, M., Stampfl, P., Mitchell, C. P., & Smith, P. (2009). Future energy potential of miscanthus in Europe. *Global Change Biology Bioenergy*, *1*, 180–196.

Hastings, A., Tallis, M., Casella, E., Matthews, R., Milner, S., Smith, P., & Taylor, G. (2014). The technical potential of Great Britain to produce lingo-cellulosic biomass for bioenergy in current and future climates. *Global Change Biology Bioenergy*, *6*, 108–122.

Hastings, A., Mos, M., Yesufu, J. A., McCalmont, J., Schwarz, K., Shafei, R., Ashman, C., Nunn, C., Schuele, H., Cosentino, S., Scalici, G., Scordia, D., Wagner, M., & Clifton-Brown, J. (2017). Economic and environmental assessment of seed and rhizome propagated *miscanthus* in the UK. *Frontiers of Plant Science*, *8*, 1058. https://doi.org/10.3389/fpls.2017.01058

Hempel, S., Frieler, K., Warszawski, L., Schewe, J., & Piontek, F. (2013). A trend-preserving bias correction – The ISI-MIP approach. *Earth System Dynamics*, *4*, 219–236. https://doi.org/10.5194/esd-4-219-2013

Huppmann, D., Rogelj, J., Kriegler, E., Krey, V., & Riahi, K. (2018). A new scenario resource for integrated 1.5°C research. *Nature*

Climate Change, *8*, 1027–1030. https://doi.org/10.1038/s41558-018-0317-4

Krause, A., Haverd, V., Poulter, B., Anthoni, P., Quesada, B., Rammig, A., & Arneth, A. (2019). Multimodel analysis of future land use and climate change impacts on ecosystem functioning. *Earth's Future*, *7*, 833–851. https://doi.org/10.1029/2018EF001123

Li, W., Ciais, P., Makowski, D., & Peng, S. (2018). A global yield dataset for major lignocellulosic bioenergy crops based on field measurements. *Scientific Data*, *5*(180), 169. https://doi.org/10.1038/sdata.2018.169

Littleton, E., Harper, A., Vaughan, N., Oliver, R., Duran-Rojas, M., & Lenton, T. (2020). JULES-BE: Representation of bioenergy crops and harvesting in the joint UKland environment simulator vn5.1. *Geoscientific Model Development*, *13*, 1123–1136. https://doi.org/10.5194/gmd-13-1123-2020

Mason, P. M., Glover, K., Smith, J. A. C., Willis, K. J., Woods, J., & Thompson, I. P. (2015). The potential of CAM crops as a globally significant bioenergy resource: Moving from 'fuel or food' to 'fuel and more food'. *Energy & Environmental Science*, *8*(8), 2320–2329. https://doi.org/10.1039/c5ee00242g

McCalmont, J., Hastings, A., Mcnamara, N., Richter, G., Robson, P., Donnison, I., & Clifton-Brown, J. (2017). Environmental costs and benefits of growing *miscanthus* for bioenergy in the UK. *GCB Bioenergy*, *9*(3), 489–507. https://doi.org/10.1111/gcbb.12294

Meinshausen, M., Raper, S. C. B., & Wigley, T. M. L. (2011). Emulating coupled atmosphere–ocean and carbon cycle models with a simpler model, MAGICC6 – Part 1: Model description and calibration. *Atmospheric Chemistry and Physics*, *11*, 1417–1456. https://doi.org/10.5194/acp-11-1417-2011

Miller, J., VanLoocke, A., Gomez-Casanovas, N., & Bernacchi, C. (2015). Candidate perennial bioenergy grasses have a higher albedo than annual row crops. *GCB Bioenergy*, *8*(4), 818–825. https://doi.org/10.1111/gcbb.12291

Muri, H. (2018). The role of large-scale BECCS in the pursuit of the 1.5°C target: An earth system model perspective. *Environmental Research Letters*, *13*, 044010. https://doi.org/10.1088/1748-9326/aab324

PBL. (2017). IMAGE 3.0 documentation online. USS manual. PBL Netherlands Environmental Assessment Agency. https://models.pbl.nl/image/index.php/USS_manual

Pogson, M., Hastings, A., & Smith, P. (2013). How does bioenergy compare with other land-based renewable energy sources globally? *GCB Bioenergy*, *5*, 513–524. https://doi.org/10.1111/gcbb.12013

Riahi, K., van Vuuren, D. P., Kriegler, E., Edmonds, J., O'Neill, B. C., Fujimori, S., Bauer, N., Calvin, K., Dellink, R., Fricko, O., Lutz, W., Popp, A., Cuaresma, J. C., Kc, S., Leimbach, M., Jiang, L., Kram, T., Rao, S., Emmerling, J., ... Tavoni, M. (2017). The shared socioeconomic pathways and their energy, land use, and greenhouse gas emissions implications: An overview. *Global Environmental Change*, *42*, 153e168. https://doi.org/10.1016/j.gloenvcha.2016.05.009

Robertson, A. D., Davies, C. A., Smith, P., Dondini, M., & McNamara, N. P. (2015). Modelling the carbon cycle of *miscanthus* plantations: Existing models and the potential for their improvement. *GCB Bioenergy*, *7*, 405–421. https://doi.org/10.1111/gcbb.12144

Rogelj, J., Luderer, G., Pietzcker, R. C., Kriegler, E., Schaeffer, M., Krey, V., & Riahi, K. (2015). Energy system transformations for limiting end-of-century warming to below 1.5°C. *Nature Climate Change*, *5*, 519–527. https://doi.org/10.1038/nclimate2572

Schaphoff, S., von Bloh, W., Rammig, A., Thonicke, K., Biemans, H., Forkel, M., Gerten, D., Heinke, J., Jägermeyr, J., Knauer, J., Langerwisch, F., Lucht, W., Müller, C., Rolinski, S., & Waha, K. (2018). LPJmL4 – A dynamic global vegetation model with managed land – Part 1: Model description. *Geoscientific Model Development*, *11*, 1343–1375. https://doi.org/10.5194/gmd-11-1343-2018

Scordia, D., Scalici, G., Clifton-Brown, J., Robson, P., Patanè, C., & Cosentino, S. L. (2020). Wild miscanthus germplasm in a drought-affected area: Physiology and agronomy appraisals. *Agronomy*, *10*, 679. https://doi.org/10.3390/agronomy10050679

Shepherd, A., Littleton, E., Clifton-Brown, J., Martin, M., & Hastings, A. (2020). Projections of global and UKbioenergy potential from *miscanthus × giganteus*—Feedstock yield, carbon cycling and electricity generation in the 21st century. *GCB Bioenergy*, *12*, 287–305. https://doi.org/10.1111/gcbb.12671

Shepherd, A., Martin, M., & Hastings, A. (2020). Uncertainty of modelled bioenergy with carbon capture and storage due to variability of input data. *GCB Bioenergy*, *13*, 691–707.

Sitch, S., Huntingford, C., Gedney, N., Levy, P. E., Lomas, M., Piao, S. I., Betts, R., Ciais, P., Cox, P., Friedlingstein, P., Jones, C. D., Prentice, I. C., & Woodward, F. I. (2008). Evaluation of the terrestrial carbon cycle, future plant geography and climate-carbon cycle feedbacks using five dynamic global vegetation models (DGVMs). *Global Change Biology*, *14*, 2015–2039. https://doi.org/10.1111/j.1365-2486.2008.01626.x

Slade, R., Bauen, A., & Gross, R. (2014). Global bioenergy resources. *Nature Climate Change*, *4*, 99–105. https://doi.org/10.1038/nclimate2097

Stehfest, E., Van Vuuren, D. P., Kram, T., & Bouwman, A. F. (2014). Integrated assessment of global environmental change with IMAGE 3.0. Model description and policy applications. In: PBL Netherlands environmental assessment agency, the Hague. http://themasites.pbl.nl/models/image/index.php/Main_Page

UNFCCC. (2015). Conference of the parties, adoption of the Paris agreement, Dec. 12, 2015, U.N. doc. FCCC/CP/2015/L.9/rev/1. https://unfccc.int/resource/docs/2015/cop21/eng/l09r01.pdf

Valentine, J., Clifton-Brown, J., Hastings, A., Robson, P., Allison, G., & Smith, P. (2011). Food vs. fuel: The use of land for lignocellulosic 'next generation' energy crops that minimise competition with primary food production. *Global Change Biology Bioenergy*, *4*, 1–19.

van Vuuren, D. P., Stehfest, E., den Elzen, M. G. J., Kram, T., van Vliet, J., Deetman, S., Isaac, M., Klein Goldewijk, K., Hof, A., Mendoza Beltran, A., Oostenrijk, R., & van Ruijven, B. (2011). RCP2.6: Exploring the possibility to keep global mean temperature increase below 2°C. *Climatic Change*, *109*, 95. https://doi.org/10.1007/s10584-011-0152-3

van Vuuren, D. P., Stehfest, E., Gernaat, D. E., van den Berg, M., Bijl, D. L., Sytze de Boer, H., Daioglou, V., Doelman, J. C., Edelenbosch, O. Y., Harmsen, M., Hof, A. F., & van Sluisveld, M. A. (2018). Alternative pathways to the 1.5°C target reduce the need for negative emission technologies. *Nature Climate Change*, *8*, 391–397. https://doi.org/10.1038/s41558-018-01198

Vaughan NE, Gough C, Mander M, Littleton EW, Welfle A, Gernaat DEHJ, van Vuuren DP (2018) Evaluating the use of biomass energy with carbon capture and storage in low emission scenarios. *Environmental Research Letters 13*(4), 044014. https://doi.org/10.1088/1748-9326/aaaa02

SUPPORTING INFORMATION

Additional supporting information can be found online in the Supporting Information section at the end of this article.